New stable donor–acceptor dyads for molecular electronics†‡

Mykola Kondratenko, Andrey G. Moiseev and Dmitrii F. Perepichka*

Received 5th August 2010, Accepted 27th September 2010
DOI: 10.1039/c0jm02545c

A series of new donor–bridge–acceptor dyads with high chemical, electrochemical, thermal and conformational stability were synthesized by Stille coupling of oligo(3,4-ethylenedioxy)thiophenes (nEDOTs) and 1,4,5,8-naphthalenetetracarboxydiimide (NDI) building blocks. The molecular design provides for complete separation of HOMO and LUMO orbitals. A thiol functionality allows for selective anchoring of the dyads to metal electrodes, through either the donor or acceptor sides of the molecule. The optoelectronic properties of the dyads, both in solution and in self-assembled monolayers on gold, were characterized by electrochemistry, spectroelectrochemistry and UV-Vis absorption/emission spectroscopy and the results were further supported by DFT calculations.

Introduction

The field of molecular electronics started with a theoretical proposal by Aviram and Ratner for electrical current rectification using a single donor–bridge–acceptor molecule. The proposed molecule was based on a stable electron donor, tetrathiafulvene (TTF) separated by a non-conjugated bridge from an electron acceptor, tetracyanoquinodimethane (TCNQ).[1] A large number of rectification studies have since been conducted for various donor–acceptor dyads, in monolayers as well as in single-molecule junctions.[2–13] The molecular origin of rectification (as opposed to that resulting from contacts with electrodes) has been clearly established in many cases. However, the applicability of this concept to the construction of practical, molecular-scale devices is still under debate.[14] Among several reasons for scepticism is lack of robustness of the resulting molecular devices, caused by chemical instability as well as positional instability of the molecules assembled in the junctions.

Intending to create simple and *stable* systems that could function as unimolecular rectifiers, we turned our attention to two well studied molecular building blocks: 1,4,5,8-naphthalenetetracarboxydiimide (NDI) and oligo(3,4-ethylenedioxythiophene) (EDOT). NDI is a planar electron-deficient molecule with exceptional chemical and thermal stability. It has been widely employed as an acceptor in model donor–acceptor dyads (used to study the fundamentals of electron transfer[15–18] and spin dynamics[19]), as a building block for *n*-channel semiconductor in organic field-effect transistors (OFETs)[20–22] and photovoltaics,[23,24] *etc.* Of particular relevance to this study, hybrid NDI-thiophene oligomers[25] and polymers[26] showed ambipolar charge-transport properties in OFETs, along with remarkable air-stability. 3,4-Ethylenedioxythiophene (EDOT) is one of the most popular electron-rich building blocks for the construction of functional conjugated materials.[27,28] The homopolymer of EDOT, PEDOT, is the most widely used and possibly the most stable known conducting polymer.[29] We thus speculated that marrying these two fragments together would provide donor–acceptor dyads with exceptionally high stability and desirable electronic properties for applications in molecular electronics. Neither EDOT nor NDI units have been employed before in molecular rectifiers.

Here, we report synthesis and detailed characterization of the electronic properties for a series of new donor–acceptor dyads NDI-EDOT (**1**), NDI-bisEDOT (**2**), RS-NDI-bisEDOT (**3**) and NDI-bisEDOT-SR (**4**) that carry NDI acceptor and EDOT donor moieties linked together through a phenyl bridge. A thiol functionality, either on the acceptor side or on the donor side, was introduced into the dyads **3** and **4** to allow covalent attachment of the molecules to gold electrodes. Corresponding self-assembled monolayers (SAMs) on gold were prepared from solution and their spectroscopic properties and electrochemical behavior were examined.

Results and discussion

Synthesis

To obtain donor–acceptor dyads with desired solubility and self-assembly functionalities the NDI acceptor and EDOT donor moieties were asymmetrically modified with linear or branched§ alkyl chains, or with a thiol-containing group. Bromine-functionalized acceptor synthons **8a,b** were prepared from a commercially available 1,4,5,8-naphthalenetetracarboxylic dianhydride **5** through a sequential reaction with corresponding primary amines to yield monoimides **6a,b** followed by condensation with 4-bromoaniline (Scheme 1). A symmetric diimide side product **7** was isolated from the synthesis of **6a** and used as a model acceptor molecule for comparative electrochemical and spectroscopic studies.

Department of Chemistry and Centre for Self-Assembled Chemical Structures, McGill University, 801 Shebrooke Str West, Montreal, Qc, H3A 2K6, Canada. E-mail: dmitrii.perepichka@mcgill.ca; Fax: +1-514-398-3797; Tel: +1-514-398-6233

† This paper is part of a *Journal of Materials Chemistry* themed issue in celebration of the 70th birthday of Professor Fred Wudl.

‡ Electronic supplementary information (ESI) available: Synthesis of intermediates; additional cyclic voltammograms; reductive spectroelectrochemistry; absorption spectra on Au substrate; TGA of **2**; NMR spectra of all compounds. See DOI: 10.1039/c0jm02545c

§ Although branched chains could prevent efficient packing of molecules in the monolayers, their presence was found necessary to achieve sufficient solubility in these dyad molecules.

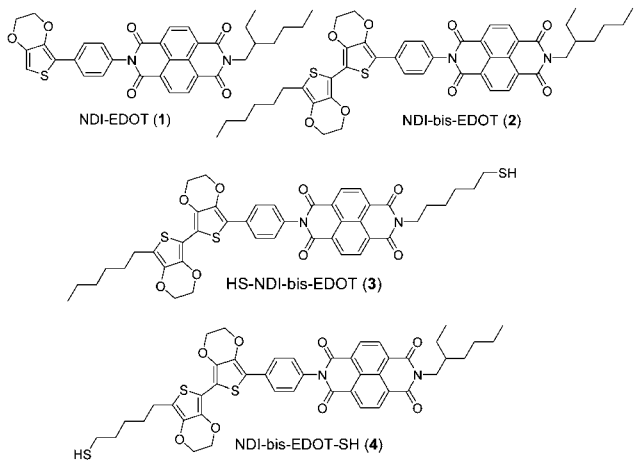

Tin-functionalized EDOT (**12**) was obtained by direct lithiation of commercial EDOT followed by coupling with tributyltin chloride. Tin-functionalized donor synthons **11a,b** were prepared by monoalkylation of a lithium salt of bisEDOT with an appropriate alkyl iodide to give the monoalkyl bisEDOT derivative **10a,b**, followed by a second lithiation and coupling with tributyltin chloride. Dihexyl-bisEDOT side product (**9**) was isolated from the synthesis of **10a** and used as a model donor compound. Similarly, alkylation of unsubstituted EDOT produced a model donor compound dihexylEDOT **13**. The final assembly of dyads **1–4** was achieved through Pd-catalyzed Stille coupling of acceptor synthons **8a,b** with donor synthons **12** or **11a,b**.

The *tert*-butyl protecting group in molecules **3a** and **4a** is necessary for successful synthesis, purification and prolonged storage of these thiol-functionalized dyads. In order to achieve grafting of the molecules on gold electrodes, the *tert*-butyl group was removed[30] at low temperature, by treatment with a strong Lewis acid (BBr_3). Then, addition of acetyl bromide to the reaction mixture led to the formation of corresponding acetylsulfanyl derivatives **3b** and **4b** that act as more stable equivalents of thiols **3** and **4** and can be attached to gold electrodes in the presence of a catalytic amount of aqueous ammonia.

Thermogravimetric analysis (TGA) showed excellent stability of the dyads: T_{dec} of 390 °C (5% loss) was measured for the model dyad **2**.

Calculations

In order to investigate the electronic structure of the prepared dyads, model molecules NDI-EDOT, NDI-bis-EDOT and NDI-tris-EDOT with methyl substituents were calculated with Density Functional Theory (DFT) at the B3LYP/6-31G(d) level of theory (Fig. 1). We were particularly interested in the energy and distribution of the HOMO and LUMO orbitals within the dyads. Optimized molecular geometries predict a large (72°) dihedral angle between the phenyl bridge and the acceptor, preventing conjugation between the donor and the acceptor. On the other hand, a moderate (18–20°) dihedral angle between the EDOT and the phenyl rings should allow substantial electron delocalization between the donor moiety and the bridge. Indeed, the orbital topology shows that the LUMO orbital is fully localized on the NDI moiety and the HOMO is mostly localized on the EDOT (bis-EDOT, tris-EDOT) fragment but partially extends on the phenyl ring (Fig. 1). The contribution of the phenyl bridge to the HOMO decreases with an increasing number of EDOT units in the donor fragment. Overall, calculations predict asymmetric distribution and complete separation of the HOMO and LUMO orbitals and confirm high rigidity of the molecules with no possibility for *intra*molecular through-space interaction between the donor and the acceptor moieties. The calculated HOMO–LUMO gap of NDI-EDOT is reduced dramatically, from 2.2 eV to 1.45 eV, upon introduction of

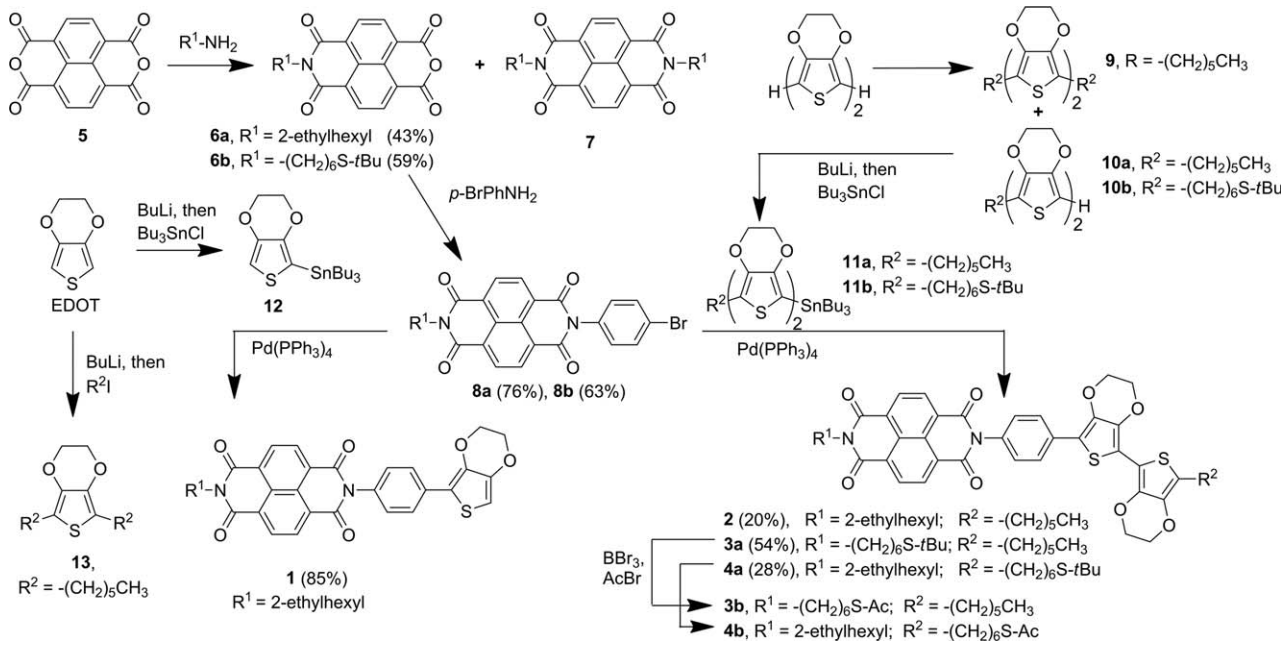

Scheme 1 Synthesis of NDI-*n*EDOT dyads.

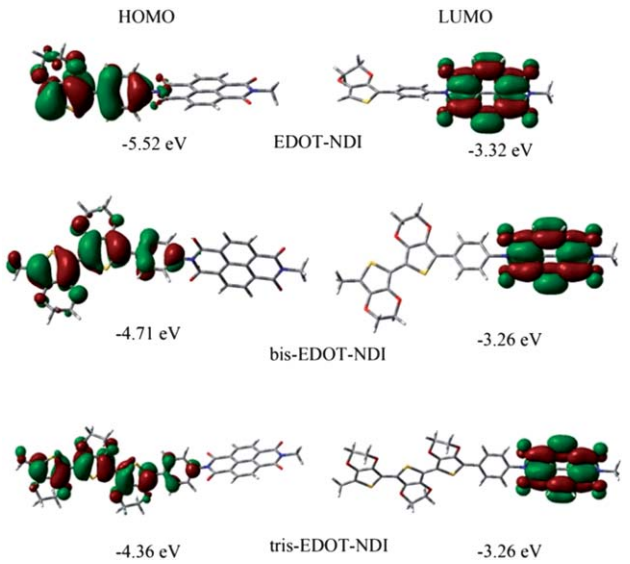

Fig. 1 Calculated molecular orbitals for nEDOT-NDI dyads.

a second EDOT ring into the donor moiety. However, adding the third EDOT ring leads to only a moderate further decrease of the gap (1.10 eV for NDI-tris-EDOT). This trend rationalizes our choice of bis-EDOT based dyads **2**, **3** and **4** as the synthetic targets of this study.

The calculations also predict a relatively low polarity of the designed dyads. The dipole moment of the NDI-bisEDOT molecule is only 2.7 D, which is drastically lower than that of the first and most extensively studied molecular rectifier $C_{16}H_{33}$Q-3CNQ (25 D).[31] We note that repulsive dipole–dipole interactions of the latter have been previously identified as one of the reasons for the low stability of molecular rectifiers based on $C_{16}H_{33}$Q-3CNQ during the measurements.[4]

Absorption/emission spectra

First, we have analyzed the UV-Vis spectra of MeCN solutions of separate donor and acceptor molecules. The model donor compounds dihexyl-EDOT (**13**) and dihexyl-bisEDOT (**9**) exhibit absorption in the UV-Vis region with maxima at 290 nm and 330 nm, respectively (Fig. 2). The vibronically structured absorption of **9** (peaks at 317, 329 and 345 nm) is indicative of the rigid structure of the bisEDOT moiety. Note that conjugation of the bisEDOT moiety with the phenyl bridge, as in dyads **2–4**, should cause a further bathochromic shift as was observed for diphenyl-bisEDOT that displays an absorption band with vibronic peaks at 375, 400, and 427 nm.[32]

The absorption spectrum of acceptor **7** is dominated by a typical for NDI strong $\pi \rightarrow \pi^*$ transition with vibronically split peaks at 342, 360, and 383 nm. The absorption spectra of the dyad molecules are essentially a superposition of absorptions of the acceptor (NDI) and the donor (phenyl-bisEDOT) moieties, showing no evidence for *intra*molecular charge-transfer in the ground state (Fig. 2). The additional shoulder at ~410 nm observed in dyad **2** but not in the NDI model **7** can be attributed to the absorption of the phenyl-bisEDOT donor moiety. Furthermore, lack of long-wavelength "charge-transfer" absorbance and no change in the absorbance spectra observed in the

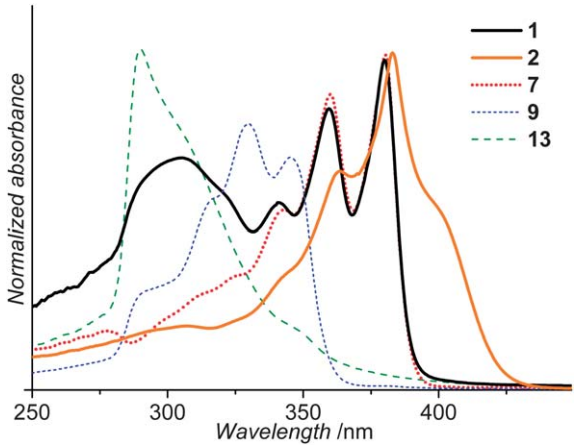

Fig. 2 UV-Vis spectra of dyads **1** and **2** and separate model donor (**9**, **13**) and acceptor model molecule (**7**) in MeCN.

wide concentration range of **2** (5×10^{-9} to 5×10^{-4} M in CH_2Cl_2) suggests that *inter*molecular charge-transfer complexation is not significant between these molecules in solution. This is in line with the relatively weak charge-transfer complexing (CTC) ability of NDI (*e.g.* association constant for CTC of *N*,*N*′-dihexyl-NDI with pyrene is 20 M^{-1}).[33] UV-Vis spectra of thin films of the dyad **2** on the glass slide (Fig. 3, black solid line) showed essentially the same absorbance as in solution, with $\lambda_{max} = 380$ nm, although an extremely weak and broad new absorption band is seen at $\lambda_{max} = 695$ nm. This weak absorption can be attributed to *inter*molecular charge transfer in the solid state (Fig. 3, in-set). Similar long wavelength absorption was observed for CTCs of *N*,*N*′-dipyridyl-NDI with other π-donors in the solid state.[34]

Study of fluorescence in MeCN solution reveals rather weak photoluminescence (PL) of the model compound **7** ($\Phi_{PL} = 0.34\%$ in CH_2Cl_2), which is slightly lowered to $\Phi_{PL} = 0.27\%$ upon attachment of the bisEDOT donor moiety in dyad **2**. It was earlier suggested that fast intersystem crossing ($\tau_{PL} = 16.4$ ps[35]) is responsible for the low fluorescence quantum yield of NDI derivatives.[20] The emission spectrum of **2** is bathochromically

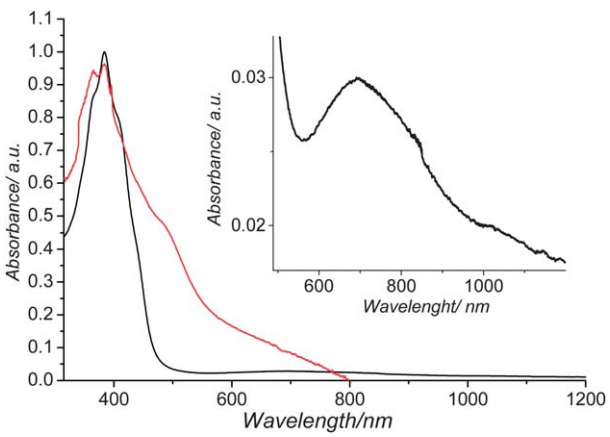

Fig. 3 Absorption spectra of a spin-coated film of the dyad **2** on glass (black, the in-set shows a magnification of the 500–1500 nm region) and SAM of the dyad **3** (red) on gold (normalized).

shifted and is broader than that of the NDI model **7** (Fig. 4). Its position is consistent with an expected emission of the phenyl-substituted bisEDOT structure.[36] This can likely be attributed to the resonance energy transfer between from NDI to bisEDOT-Ph fragments in the dyad **2** since the absorbance of the bisEDOT-Ph moiety (shoulder at 410 nm) overlaps with the emission of the NDI moiety. Such energy transfer was not observed in the dyad **1** (Fig. 4), where the absorbance of the EDOT-Ph moiety occurs at higher energy. We note that bathochromically shifted emission was also observed for NDI derivatives in low-polarity solvents like toluene (but never in high-polarity solvents like MeCN) and it was attributed to formation of NDI excimers.[37] We also have observed such "excimer" emission for the model NDI **7** (as well for the dyad **2**) in toluene, at a higher wavelength ~500 nm (see ESI‡). However, in MeCN, an expected monomeric NDI fluorescence band (~400 nm) was the only observed emission for the model NDI **7** and the dyad **1**.

Electrochemistry

The electrochemical behavior of the synthesized molecules was studied using cyclic voltammetry (Fig. 5, Table 1). All NDI derivatives showed two well-separated, reversible, one-electron reduction waves corresponding to the formation of the radical anion and dianion. The reduction potentials of dyads **1** and **2** were slightly less negative than those of the model acceptor **7** and did not depend on the nature of the donor moiety. This can be attributed to the slightly electron withdrawing effect of the phenyl bridge, in comparison with the electron donating nature of the alkyl group. The one-electron oxidation corresponding to formation of a radical cation on the nEDOT fragment was electrochemically irreversible. The corresponding oxidation potential decreases by ~600 mV upon addition of the second EDOT unit in the donor fragment (**1** → **2**), whereas the reduction potentials stay practically unaffected. The HOMO and LUMO values deduced from electrochemistry (Table 1) are in good agreement with values calculated by DFT (Fig. 1).

The electrochemically-irreversible nature of the oxidation requires a special discussion in light of our aim to create highly stable donor–acceptor dyads. Such behavior was also observed

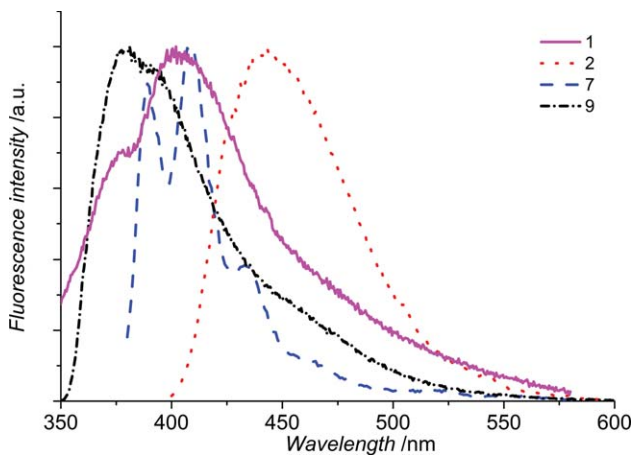

Fig. 4 Normalized emission spectra of the dyads **1** and **2**, NDI acceptor **7** and bisEDOT donor **9** in MeCN (excitation at 340 nm).

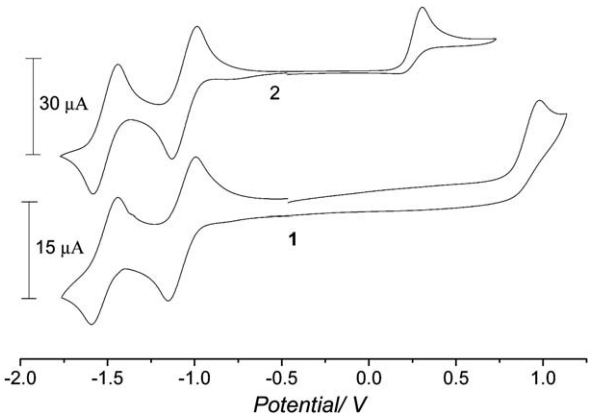

Fig. 5 Cyclic voltammogram of **1** and **2** in CH_2Cl_2 *vs.* Fc/Fc^+.

for model dihexyl-EDOT **13** and dihexyl-bisEDOT **9** (ESI‡) and was previously speculated to be due to dimerization of the radical cations formed.[38] To prove the nature of the oxidized species we have performed bulk electrolysis of the model donor **9**. The experiment was done in the electrochemical cell for bulk electrolysis in degassed MeCN solution by applying constant potential at 1.0 V for 20 min. The analysis of EPR spectra of the oxidized species showed no radical species present in solution. UV-Vis spectroelectrochemical studies in dry, degassed MeCN reveal that upon gradual increase of the redox potential, the absorption of the neutral molecule in the 300–360 nm region is gradually replaced by a new absorption in the 360–500 nm region, with clear isosbestic points at 258 and 355 nm (Fig. 6). The absorption of oxidized species grows rapidly (the equilibrium is reached within ~1–2 min at each new potential value). During the backward reduction of the product, disappearance of the absorbance band at 360–500 nm and recovery of the original spectrum occurs at much slower rate (15–20 min required to reach the equilibrium after each change of the potential). Such slow reduction explains the irreversible CV. Nevertheless, the neutral molecule can be fully recovered upon reversal of the potential. A small additional shoulder at ~520 nm which is visible on the forward (oxidative) direction but which quickly disappears and is not observed during the reduction sweep, is likely due to absorption of the radical cation transient. Based on the above observation, the overall process appears as depicted in Scheme 2. An electron transfer from **9** onto the electrode forming the radical cation is followed by a fast dimerization process to give the bisEDOT dimer dication $(\mathbf{9})_2^{2+}$. Two-electron reduction

Table 1 Electrochemical data for the synthesized dyads and model donor and acceptor compounds

	E^0_{1red}, V	E^0_{2red}, V	E^{pa}_{1ox}, V	HOMO,[a] eV	LUMO,[b] eV	Gap, eV
1	−1.06	−1.51	0.98	−5.8	−3.7	2.0
2	−1.07	−1.52	0.31	−5.1	−3.7	1.4
7	−1.13	−1.59	—			
9	—	—	0.36			
13			0.97			

[a] Determined from anodic oxidation peak (vs Fc/Fc^+) using the equation (HOMO = $-4.8 - E^a_{ox}$). [b] Determined from the first reduction peak (vs Fc/Fc+) using the equation (LUMO = $-4.8 - E_{1/2}{}^1_{red}$).

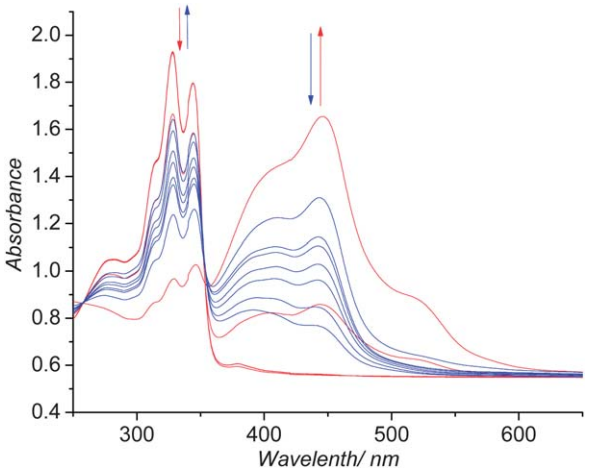

Fig. 6 Spectroelectrochemistry of the bisEDOT **9** in MeCN; red: oxidation, blue: reduction.

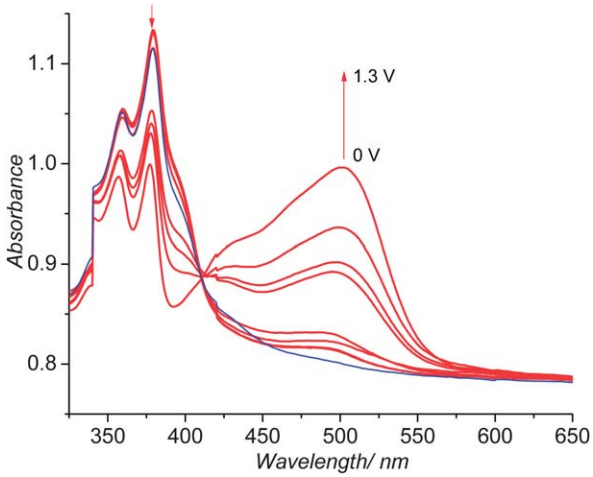

Fig. 7 Spectroelectrochemistry of the dyad **2** in MeCN (blue line shows restoration of the original spectrum after reduction of the oxidized solution at −0.2 V).

of this dication, which leads to recovery of the neutral monomeric **9**, however, is a slow process that leads to an electrochemically-irreversible CV signature.

Similar results were obtained in spectroelectrochemical study of the dyad **2** (Fig. 7). Neutral **2** exhibits absorption at 325–420 nm region, which is an overlap of the donor and acceptor absorption bands. Upon gradual increase of the oxidation potential, from 0 to 1.3V, a new absorption band of the oxidized species appears at $\lambda_{max} = 505$ nm. The shoulder at ~400 nm corresponding to the bisEDOT moiety attenuates but the vibronically-split band of NDI at 380 nm persists. Electrochemical reduction back to the neutral state leads to complete disappearance of the oxidized species and restores the pristine absorption of the neutral **2**. We speculate that such behavior could give rise to bistable switching characteristics in the transport properties of the molecular junctions based on dyads **2**, although the kinetics of dimer dissociation appear too slow for practical applications.

We have also studied cathodic (reductive) electrochemistry of the dyad **2** which has revealed characteristic spectral features (at $\lambda_{max} = 460$, 610, 700 and 780 nm) that have been earlier reported for radical anion of dialkyl-NDI[15] (ESI‡).

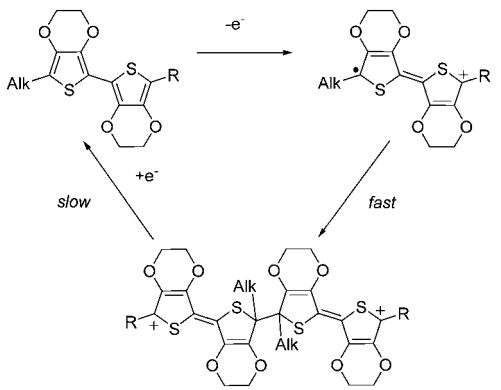

Scheme 2 Proposed scheme of the reversible oxidative dimerization of bisEDOT derivatives.

SAM preparation and characterization

The thiol functionality on either the donor or acceptor part of dyads **3** and **4** allows covalent attachment of the molecules to the gold surface. Monolayers of Au-S-NDI-bisEDOT and Au-S-bisEDOT-NDI were prepared *via* self-assembly of acetyl-protected molecules **3b** and **4b**, respectively, onto evaporated gold substrates from THF solution, in the presence of a catalytic amount of NH_4OH. Freshly prepared SAMs were characterized by grazing angle FT-IR and UV-Vis spectroscopy, ellipsometry, contact angle and electrochemical measurements.

Ellipsometry indicates that the thickness of the SAMs of **3** and **4** are 31 ± 2 Å and 26 ± 2 Å, respectively. This agrees well with the calculated length of the molecules (34 Å) and suggests an essentially upright (with a small tilt) orientation on the surface. Static contact angle measurements (70° ± 2° for dyad **3** and 75° ± 2° for dyad **4**) indicate that the surface of the SAMs is relatively hydrophobic. Compared to the 110° contact angle for highly ordered and very dense monolayers of the alkyl thiols, we can conclude that terminal alkyl tails of **3** and **4** in neat SAMs are loosely packed. This is not unexpected, considering the twisted geometry of the core. A slightly more hydrophobic surface for dyad **3** can be attributed to the branched 2-ethylhexyl tail that fully covers a polar NDI fragment.

Grazing incidence angle FT-IR spectra of the SAMs studied on planar gold mirror substrates shows the same features as those of the bulk, proving the preservation of the molecular structure in the monolayer (Fig. 8). The characteristic C=O vibration of the two imide groups appears at 1670 cm^{-1} and 1709 cm^{-1} in the spectra of the SAMs. The frequencies of CH_2 stretching modes at 2930 and 2858 cm^{-1} are higher than those of densely packed SAMs of normal long-chain alkanethiols [ν_{as} (CH_2) = 2917 cm^{-1}, ν_s (CH_2) = 2849 cm^{-1}], indicating a significant disorder of alkyl chains of **3** and **4** in SAMs.[39,40]

UV-Vis absorption of SAMs of dyad **3** were studied on thin, semi-transparent, gold-coated (~50 nm) microscope glass slides. The spectrum of a freshly prepared SAM of **3** presents a characteristic peak at 380 nm, fully resembling that of **2** in spin-coated films (Fig. 3). An additional weak shoulder at ~500 nm

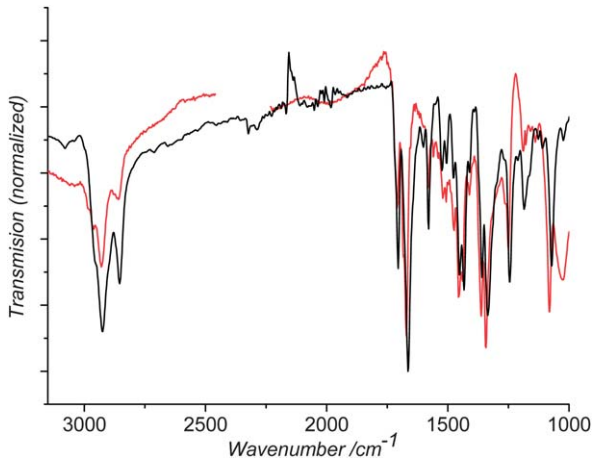

Fig. 8 ATR FTIR of the bulk (black) and GA-FTIR of the monolayer on gold (red) of **3** (all spectra are normalized).

can be attributed to a plasmonic band of gold nanoislands in thin, vacuum-coated gold films (see also ESI‡).[41] Its interference precludes us from assessing a possible weak charge-transfer band in the SAMs.

Cyclic voltammetry of the SAMs of the dyads **3** and **4** resembles that of solution experiments (Fig. 9). Two reversible reduction waves, characteristic of the NDI fragment, appear at E^0_{red} 1.08 and 1.55 V *vs.* Fc/Fc^+, respectively. A partially reversible oxidation peak due to the bisEDOT fragment is observed at $E^{pa}_{ox} = 0.46$ V *vs.* Fc/Fc^+. Multiple scanning of the SAMs through the first reduction wave (formation of the radical anion) shows moderate stability with a 20–30% drop of the current after 50 cycles in the range of 0 to −0.8 V (see ESI‡). This can be attributed to desorption of the molecules from the surface due to repulsion of the positively charged molecules. The peak current scales linearly (ESI‡) with the scan rate, indicating a surface-confined nature of the process.

The surface coverage (Γ) was calculated from the CV peak area. An average value for SAMs calculated from anodic peaks is 4.2×10^{-10} mol/cm^2 for dyad **3** and 1.6×10^{-10} mol/cm^2 for dyad **4**, which correspond to average molecular areas of 40 Å^2 and 110 Å^2 respectively. Comparing these values with the results reported for SAMs of TCNQ (3–3.5 $\times$ 10^{-10} mol/cm^2),[42] TTF-thioctic ester (2.1 $\times$ 10^{-10} mol/cm^{-10}),[43] fluorene-thioctic ester (3.5 $\times$ 10^{10} mol/cm^2)[44] and considering twisted geometry of the molecules we can conclude that the dyad **3** forms well packed monolayers of "stand-up" molecules. The larger molecular area for dyad **4** can be explained by a more bulky 2-ethylhexyl tail on the NDI fragment that leads to less dense packing, and is consistent with the lower thickness of SAMs of **4** observed by ellipsometry (see above).

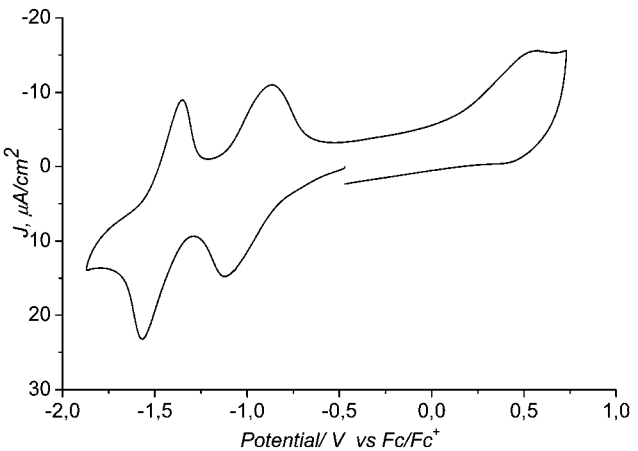

Fig. 9 Cyclic voltammogram of a SAM of **3**; electrolyte 0.2 M Bu_4NPF_6 in CH_2Cl_2.

Conclusions

New donor–acceptor dyads based on highly stable bis-EDOT donor and NDI acceptor moieties have been synthesized. A thiol functionality on either the donor or the acceptor parts enables anchoring of the dyads to a gold electrode in two different orientations. The rigid geometry of the molecular core and a large twist between the acceptor and the phenylene bridge allows for efficient separation of the HOMO and LUMO orbitals, despite their close proximity. Accordingly, no donor–acceptor interactions occur in these dyads in the ground state. The HOMO–LUMO gap of ~1.4 eV provides for sufficient chemical and electronic stability,[45] while a low dipole moment of ~2.7 D is expected to lead to orientational stability of the molecules in monolayer junctions. The study of their transport properties as rectifiers in molecular junctions is currently under way. A chemically reversible dimerization of the bis-EDOT moieties, established through spectroelectrochemistry and EPR spectroscopy, offers potential additional opportunity for the design of molecular switches based on NDI-bis-EDOT dyads.

Experimental part

Cyclic voltammetry

Cyclic voltammetry measurements were done using a CHI-670 potentiostat under nitrogen in a CH_2Cl_2 solution of electrolyte (0.1 M Bu_4NPF_6) with a Ag/AgCl reference electrode and platinum disk (d = 1.6 mm) as a working electrode for solution experiments and a gold disk electrode (BAS, d = 1.6 mm) for the SAM experiments. Fc/Fc^+ (0.50 V *vs.* Ag/AgCl in these conditions) was used as an internal reference.

Calculations

Calculations of geometry and electronic structure of the dyads were done using density functional theory (DFT) with hybrid B3LYP functional and 6-31G(d) basis set, as implemented in Gaussian W03.[46] The alkyl substituents on both donor and acceptor moieties were modeled using methyl groups.

Absorbance/emission spectroscopy

Absorption spectra were recorded with a Jasco V-670 spectrophotometer in CH_2Cl_2 and MeCN solutions. Fluorescence was recorded on Cary Eclipse fluorimeter in MeCN and toluene solutions. For measurements of the solid state samples, two kinds of samples were prepared: 1) spin-coated thin film of **2** on a clean glass slide (a similar clean glass slide was used as

a reference); 2) self-assembled monolayer of **3** and **4** on very thin (≤50 nm) gold film, evaporated on a glass slide. A part of this slide, without the SAM, was used as a reference.

FTIR spectroscopy

FTIR spectra were recorded with a Nicolet 6700 FTIR spectrometer equipped with a liquid-N_2-cooled MCT-II detector with spectral resolution of 4 cm^{-1}. ATR mode (Smart-Orbit accessory, diamond crystal) was used for bulk samples, and grazing angle (80°) reflectance-absorbance mode (RAIRS), using a grazing angle Smart-SAGA accessory, was employed for SAMs on gold. The measurements were done in an atmosphere of dry, CO_2-free air, and an identical gold-coated slide (prepared in the same Au evaporation run, stored under methanol and cleaned with air plasma before use) was used as a reference.

Ellipsometry

SAM thicknesses were measured on a ellipsometer equipped with a He–Ne laser ($\lambda = 632.8$ nm) at an incidence angle of 70° with respect to the surface normal. Optical constants of the gold-coated substrates were measured using a bare gold slide (Ns = 0.25, Ks = −3.46). The reference sample was cleaned by soaking in HPLC dichloromethane and air plasma treated immediately before the measurements. The layer thickness was calculated by averaging over 10 measurements. The refractive index of the monolayer was assumed to be 1.46.

Contact angle measurements

The static contact angles of deionized water (>18 MΩ cm) were measured on a homemade contact angle goniometer and averaged over 3–5 spots. The plasma-cleaned Au surface produced a static contact angle of 0°.

Spectroelectrochemistry

Spectroelectrochemistry experiments were performed in a thin layer spectroelectrochemical cell CHI140A from CH Instruments equipped with a platinum grid as a working, platinum wire as a counter and Ag/AgCl as a reference electrode. UV-Vis spectra were recorded with a Jasco V-670 spectrophotometer and a BASF Epsilon potentiostat and the static potential mode was used for oxidation/reduction of the molecules. Potentials were applied in 50–100 mV steps and equilibrated by allowing the current to drop until a negligible current change was achieved (less than 1% of initial current per minute).

SAM preparation

Slides of gold, evaporated on a silicon wafer or glass substrate were immersed in a 10^{-3} M solution of the NDI-bis-EDOT dyads for 12–48 h. After that period gold slides were washed with THF with sonication for a few seconds and dried under vacuum.

Synthetic procedures for 6a, 6b, 7, 8a, 8b, 10a, 10b, 11a, 11b, 12, 13 and all *tert*-butylsulfanyl-containing reagents are given in the ESI.‡

NDI-EDOT dyad (1)

To a solution of NDI **8a** (0.50 g, 0.94 mmol) and 2-tributylstannyl-EDOT[38] **12** (0.50 g, 1.2 mmol) in dry toluene under nitrogen atmosphere was added a catalyst $Pd(PPh_3)_4$ (0.054 g, 0.05 mmol), and the reaction mixture was stirred at reflux for 12 h. After all starting compound **8a** had reacted, the mixture was cooled and the solvent was evaporated under reduced pressure. The residue was dissolved in CH_2Cl_2 and washed with water and brine, and the organic phase was dried over $MgSO_4$. Purification by column chromatography on silica using CH_2Cl_2 as an eluent afforded desired product **1** as an orange solid (0.47 g, 85%). M.p. 220–222 °C; δ_H (400 MHz, $CDCl_3$) 8.82 (2H, d, 8 Hz), 8.79 (2H, d, 7.6 Hz), 7.91 (2H, d, *J* 8.8 Hz), 7.31 (2H, d, *J* 8.8 Hz), 6.36 (1H, s), 4.26 (4H, m), 4.17 (2H, m), 1.92 (1H, m), 1.36 (8H, m), 0.95 (3H, t, *J* 7.4 Hz), 0.89 (3H, t, *J* 7.2 Hz); δ_C (75.0 MHz, $CDCl_3$) 163.2, 163.0, 142.2, 138.8, 134.2, 132.4, 131.4, 131.1, 128.6, 127.06, 126.95, 126.89, 126.86, 126.68, 116.5, 98.4, 64.8, 64.4, 44.7, 37.9, 30.7, 28.6, 24.0, 23.0, 14.1, 10.6; HR-MS (ESI): calculated for $C_{34}H_{31}N_2O_6S$ (M + 1) 595.1897, found 595.1880.

NDI-bis-EDOT dyad (2)

To a solution of NDI **8a** (0.82 g, 1.52 mmol) and 5-tributylstannyl-5′-hexyl-bis-EDOT (1.00 g, 1.52 mmol) in dry toluene (20 ml) under nitrogen atmosphere was added a catalyst $Pd(PPh_3)_4$ (0.088 g, 0.076 mmol) and the reaction mixture was stirred at 110 °C for 24 h. After all starting compounds had reacted as monitored by TLC (silica, CH_2Cl_2), the reaction was cooled and the solvent was evaporated under reduced pressure. The residue was redissolved in CH_2Cl_2, washed with water and brine, and the organic phase was dried over $MgSO_4$. Column chromatography on silica eluting with CH_2Cl_2 resulted in product **2** as a dark green solid (0.25 g, 20%). M.p. 305–306 °C; δ_H (400 MHz, $CDCl_3$) 8.75 (2H, d, 7.6 Hz), 8.73 (2H, d, 7.6 Hz), 7.87 (2H, d, *J* 8.8 Hz), 7.28 (2H, d, *J* 8.8 Hz), 4.36–4.22 (8H, m), 4.15 (2H, m), 2.64 (2H, t, *J* 7.6 Hz), 1.96 (1H, m), 1.61 (2H, m), 1.35 (14H, m), 0.95 (3H, t, *J* 7.4 Hz), 0.89 (6H, m, *m*); δ_C (75.0 MHz, $CDCl_3$) 163.2, 163.0, 138.6, 137.2, 137.1, 136.5, 134.2, 131.9, 131.3, 130.9, 128.5, 127.0, 126.80, 126.77, 126.6, 126.5, 117.4, 112.9, 109.5, 105.4, 65.2, 64.7, 64.5, 44.6, 37.9, 31.6, 30.7, 30.5, 28.9, 28.6, 25.8, 24.0, 23.1, 22.6, 14.1, 10.6; HR-MS (ESI): calculated for $C_{46}H_{46}N_2O_8S_2$ 818.2696, found 818.2680.

NDI-bis-EDOT dyad (4a)

To a solution of NDI **8a** (0.070 g, 0.134 mmol) and 5-tributylstannyl-5′-(6-(*tert*-butylsulfanyl)hexyl)-bis-EDOT (0.1 g, 0.134 mmol) in dry toluene under nitrogen atmosphere was added catalyst $Pd(PPh_3)_4$ (0.010 g, 0.007 mmol), and the reaction mixture was stirred at 85 °C for 24 h. After all starting material had reacted (followed by TLC on silica), the reaction was cooled and the solvent was evaporated under reduced pressure. The residue was dissolved in CH_2Cl_2 and washed with water and brine, then the organic phase was dried with $MgSO_4$. Column chromatography on silica with CH_2Cl_2 as an eluent resulted in desired product **4a** as a dark green solid (0.035 g, 28%). M.p. 272–274 °C; δ_H (400 MHz, $CDCl_3$) 8.81 (2H, d, 7.5 Hz), 8.79 (2H, d, 7.5 Hz), 7.92 (2H, d, *J* 8.4 Hz), 7.29 (2H, d, *J* 8.4 Hz), 4.49–4.15

(8H, m), 4.16 (2H, m), 2.66 (2H, t, *J* 7.5 Hz), 2.52 (2H, t, *J* 7.2 Hz), 1.96 (1H, m), 1.70–1.50 (4H, m), 1.50–1.35 (14H, m), 1.31 (9H, s), 0.95 (3H, t, *J* 7.4 Hz), 0.89 (3H, t, *J* 7.2 Hz); δ_C (125.0 MHz, $CDCl_3$) 163.2, 163.0, 138.6, 137.3, 136.6, 134.3, 131.9, 131.4, 131.1, 128.5, 127.0, 126.9, 126, 7, 126.6, 117.0, 113.1, 109.5, 105.6, 65.2, 64.8, 64.5, 44.7, 37.9, 31.0 30.70, 30.66, 30.2, 29.4, 29.1, 28.64, 28.56, 28.50, 25.7, 24.0, 23.0, 14.1, 10.6; HR-MS (ESI): calculated for $C_{50}H_{54}N_2O_8S_3$ 906.3042, found: 906.3037.

NDI-bis-EDOT dyad (4b)

To a solution of *tert*-butyl protected dyad **4a** (0.035 g, 0.039 mmol) in dry CH_2Cl_2 (15 ml) at −78 °C was added acetyl bromide (0.2 ml, excess) followed by 0.1 M solution of BBr_3 in CH_2Cl_2 (0.8 ml, 0.08 mmol) under nitrogen atmosphere. The reaction mixture was stirred at room temperature for 4 h and poured into ice. The resulted solution was extracted with CH_2Cl_2. The organic phase was separated and washed with water, brine, and dried over $MgSO_4$. Crude product was recrystallized from CH_2Cl_2–hexanes to afford green solid **4b** (0.018 g, 52%). M.p. 290–293 °C. δ_H (400 MHz, $CDCl_3$) 8.82 (2H, d, 7.6 Hz), 8.79 (2H, d, 7.6 Hz), 7.93 (2H, d, *J* 8.4 Hz), 7.29 (2H, d, *J* 8.4 Hz), 4.5–4.2 (8H, m), 4.18 (2H, m), 2.86 (2H, t, *J* 7.2), 2.65 (2H, t, *J* 7.2), 2.32 (3H, s), 1.97 (1H, m), 1.71–1.50 (4H, m), 1.50–1.20 (14H, m), 0.96 (3H, t, *J* 7.4 Hz), 0.90 (3H, t, *J* 7.2 Hz); δ_C (125.0 MHz, $CDCl_3$) 163.2, 163.0, 138.6, 137.3, 136.6, 134.3, 131.9, 131.4, 131.1, 128.5, 127.0, 126.9, 126, 7, 126.6, 117.0, 113.1, 109.5, 105.6, 65.2, 64.8, 64.5, 44.7, 37.9, 30.70, 30.66, 30.2, 29.4, 29.1, 28.64, 28.56, 28.50, 25.7, 24.0, 23.0, 14.1, 10.6; HR-MS (ESI): calculated for $C_{48}H_{48}O_9N_2S_3$ 892.2522, found 892.2526.

NDI-bis-EDOT dyad (3a)

To a solution of NDI **8b** (0.30 g, 0.48 mmol) and **11a**[38] (see ESI‡) (0.34 g, 0.52 mmol) in dry toluene under nitrogen atmosphere was added catalyst $Pd(PPh_3)_4$ (0.030 g, 0.025 mmol), and the reaction mixture was stirred at reflux for 6 h. After all starting compound had reacted (followed by TLC, silica, eluent CH_2Cl_2), the reaction was cooled and the solvent was evaporated under reduced pressure. The residue was purified by column chromatography on silica (eluent: CH_2Cl_2, followed by 20 : 1 CH_2Cl_2–EtOAc) resulting in the desired compound **3a** as a dark green solid (0.255 g, 54% yield). M.p. 330–333 °C; δ_H (400 MHz, $CDCl_3$) 8.81 (2H, d, 6 Hz), 8.79 (2H, d, 7.6 Hz), 7.92 (2H, d, *J* 8.4Hz), 7.29 (2H, d, *J* 8.4 Hz), 4.5–4.1 (10H, m), 2.65 (2H, t, *J* 7.2), 2.53 (2H, t, *J* 7.2), 1.77 (2H, br), 1.63 (m, 4H), 1.49 (m, 2H), 1.36 (t, br, 2H), 1.32 (s, 9H), 0.89 (t, 3H, *J* 7.0 Hz); δ_C (75.0 MHz, $CDCl_3$) 163.1, 162.8, 138.6, 137.3, 137.1, 136.6, 134.3, 131.9, 131.4, 131.0, 128.5, 127.0, 126.9, 126.8, 126.7, 126.6, 117.4, 113.0, 109.5, 105.5, 65.2, 64.8, 64.5, 41.8, 40.9, 31.6, 31.0, 30.5, 29.7, 29.0, 28.9, 28.2, 28.0, 26.8, 25.8, 22.6, 14.1. HR-MS (ESI): calculated for $C_{48}H_{50}O_8N_2S_3$ 878.2729, found 878.2737.

NDI-bis-EDOT dyad (3b)

To a solution of *tert*-butyl protected dyad **3a** (0.093 g, 0.1 mmol) in dry CH_2Cl_2 (30 mL) at −78 °C and acetyl bromide (0.1 ml) was added 0.1 M solution of BBr_3 in CH_2Cl_2 (1 mL, 0.1 mmol) dropwise and the reaction mixture was slowly warmed to room temperature. After stirring for 4 h the reaction was quenched with water and the crude product was extracted with CH_2Cl_2. The organic phase was washed with water, brine and dried with $MgSO_4$. Purification by column chromatography on silica (CH_2Cl_2:EtOAc eluent, gradient) gave the desired product as a green solid (0.047 g, 51%). M.p. 291–294 °C. δ_H (500 MHz, $CDCl_3$) 8.82 (2H, d, 7.5 Hz), 8.79 (2H, d, 7.5 Hz), 7.92 (d, 2H, *J* 9.0 Hz), 7.29 (d, 2H, *J* 9.0 Hz), 4.42–4.20 (m, 10H), 2.86 (t, 2H, *J* 7.5), 2.33 (s, 3H), 1.76 (m, 2H), 1.57–1.45 (m, 2H), 1.45–1.20 (m, 14H) 0.92 (t, 3H, *J* 7.5 Hz); δ_C (125.0 MHz, $CDCl_3$) 196.0, 163.0, 162.8, 138.6, 137.3, 137.2, 137.1, 134.1, 132.1, 131.3, 130.9, 128.5, 127.0, 126.81, 126.78, 126.68, 126.58, 126.52, 118.9, 115.5, 113.7, 109.4, 106.4, 65.2, 64.7, 64.6, 40.9, 32.9, 31.5, 30.6, 29.4, 29.1, 29.0, 28.9, 28.7, 28.7, 28.0, 26.9, 22.6, 22.2, 13.9. HRMS (ESI) calculated for $C_{46}H_{44}O_9N_2S_3$ 864.2209 found 864.2219.

Acknowledgements

This work was funded by NSERC Discovery and Strategic grants and infrastructure LOF grant from CFI. Support from the FQRNT Centre for Self-Assembled Chemical Structures is also acknowledged.

Notes and references

1 A. Aviram and M. A. Ratner, *Chem. Phys. Lett.*, 1974, **29**, 277–283.
2 R. M. Metzger, *Chem. Rev.*, 2003, **103**, 3803–3834.
3 G. J. Ashwell, J. R. Sambles, A. S. Martin, W. G. Parker and M. Szablewski, *J. Chem. Soc., Chem. Commun.*, 1990, 1374–1376.
4 R. M. Metzger, B. Chen, U. Hopfner, M. V. Lakshmikantham, D. Vuillaume, T. Kawai, X. L. Wu, H. Tachibana, T. V. Hughes, H. Sakurai, J. W. Baldwin, C. Hosch, M. P. Cava, L. Brehmer and G. J. Ashwell, *J. Am. Chem. Soc.*, 1997, **119**, 10455–10466.
5 A. C. Brady, B. Hodder, A. S. Martin, J. R. Sambles, C. P. Ewels, R. Jones, P. R. Briddon, A. M. Musa, C. A. F. Panetta and D. L. Mattern, *J. Mater. Chem.*, 1999, **9**, 2271–2275.
6 R. M. Metzger, T. Xu and I. R. Peterson, *J. Phys. Chem. B*, 2001, **105**, 7280–7290.
7 R. M. Metzger, J. W. Baldwin, W. J. Shumate, I. R. Peterson, P. Mani, G. J. Mankey, T. Morris, G. Szulczewski, S. Bosi, M. Prato, A. Comito and Y. Rubin, *J. Phys. Chem. B*, 2003, **107**, 1021–1027.
8 P. Jiang, G. M. Morales, W. You and L. P. Yu, *Angew. Chem., Int. Ed.*, 2004, **43**, 4471–4475.
9 G. J. Ashwell, A. Chwialkowska and L. R. H. High, *J. Mater. Chem.*, 2004, **14**, 2848–2851.
10 G. J. Ashwell, A. Chwialkowska and L. R. H. High, *J. Mater. Chem.*, 2004, **14**, 2389–2394.
11 G. M. Morales, P. Jiang, S. W. Yuan, Y. G. Lee, A. Sanchez, W. You and L. P. Yu, *J. Am. Chem. Soc.*, 2005, **127**, 10456–10457.
12 G. Ho, J. R. Heath, M. Kondratenko, D. F. Perepichka, K. Arseneault, M. Pezolet and M. R. Bryce, *Chem.–Eur. J.*, 2005, **11**, 2914–2922.
13 G. J. Ashwell, B. Urasinska-Wojcik and L. J. Phillips, *Angew. Chem., Int. Ed.*, 2010, **49**, 3508–3512.
14 R. M. Metzger, *Synth. Met.*, 2009, **159**, 2277–2281.
15 S. V. Bhosale, C. H. Jani and S. J. Langford, *Chem. Soc. Rev.*, 2008, **37**, 331–342.
16 H. Levanon, T. Galili, A. Regev, G. P. Wiederrecht, W. A. Svec and M. R. Wasielewski, *J. Am. Chem. Soc.*, 1998, **120**, 6366–6373.
17 K. Hasharoni, H. Levanon, S. R. Greenfield, D. J. Gosztola, W. A. Svec and M. R. Wasielewski, *J. Am. Chem. Soc.*, 1996, **118**, 10228–10235.
18 M. P. Debreczeny, W. A. Svec, E. M. Marsh and M. R. Wasielewski, *J. Am. Chem. Soc.*, 1996, **118**, 8174–8175.

19 Q. X. Mi, E. T. Chernick, D. W. McCamant, E. A. Weiss, M. A. Ratner and M. R. Wasielewski, *J. Phys. Chem. A*, 2006, **110**, 7323–7333.
20 H. E. Katz, A. J. Lovinger, J. Johnson, C. Kloc, T. Siegrist, W. Li, Y. Y. Lin and A. Dodabalapur, *Nature*, 2000, **404**, 478–481.
21 B. A. Jones, A. Facchetti, T. J. Marks and M. R. Wasielewski, *Chem. Mater.*, 2007, **19**, 2703–2705.
22 D. Shukla, S. F. Nelson, D. C. Freeman, M. Rajeswaran, W. G. Ahearn, D. M. Meyer and J. T. Carey, *Chem. Mater.*, 2008, **20**, 7486–7491.
23 W. J. Grzegorczyk, P. Ganesan, T. J. Savenije, S. van Bavell, J. Loos, E. J. R. Sudholter, L. D. A. Siebbeles and H. Zuilhof, *J. Phys. Chem. C*, 2009, **113**, 7863–7869.
24 M. A. Angadi, D. Gosztola and M. R. Wasielewski, *J. Appl. Phys.*, 1998, **83**, 6187–6189.
25 R. P. Ortiz, H. Herrera, R. Blanco, H. Huang, A. Facchetti, T. J. Marks, Y. Zheng and J. L. Segura, *J. Am. Chem. Soc.*, 2010, **132**, 8440–8452.
26 H. Yan, Z. H. Chen, Y. Zheng, C. Newman, J. R. Quinn, F. Dotz, M. Kastler and A. Facchetti, *Nature*, 2009, **457**, 679–U671.
27 B. L. Groenendaal, F. Jonas, D. Freitag, H. Pielartzik and J. R. Reynolds, *Adv. Mater.*, 2000, **12**, 481–494.
28 J. Roncali, P. Blanchard and P. Frere, *J. Mater. Chem.*, 2005, **15**, 1589–1610.
29 S. Kirchmeyer and K. Reuter, *J. Mater. Chem.*, 2005, **15**, 2077–2088.
30 N. Stuhr-Hausen, *Synth. Commun.*, 2003, **33**, 641–646.
31 R. M. Metzger, *J. Mater. Chem.*, 2000, **10**, 55–62.
32 J. J. Apperloo, L. Groenendaal, H. Verheyen, M. Jayakannan, R. A. J. Janssen, A. Dkhissi, D. Beljonne, R. Lazzaroni and J. L. Bredas, *Chem.–Eur. J.*, 2002, **8**, 2384–2396.
33 T. C. Barros, S. Brochsztain, V. G. Toscano, P. Berci and M. J. Politi, *J. Photochem. Photobiol., A*, 1997, **111**, 97–104.
34 D. R. Trivedi, Y. Fujiki, Y. Goto, N. Fujita, S. Shinkai and K. Sada, *Chem. Lett.*, 2008, **37**, 550–551.
35 Y. Posokhov, S. Alp, B. Koz, Y. Dilgin and S. Icli, *Turk. J. Chem.*, 2004, **28**, 415–424.
36 D. Wasserberg, P. Marsal, S. C. J. Meskers, R. A. J. Janssen and D. Beljonne, *J. Phys. Chem. B*, 2005, **109**, 4410–4415.
37 G. Andric, J. F. Boas, A. M. Bond, G. D. Fallon, K. P. Ghiggino, C. F. Hogan, J. A. Hutchison, M. A. P. Lee, S. J. Langford, J. R. Pilbrow, G. J. Troup and C. P. Woodward, *Aust. J. Chem.*, 2004, **57**, 1011–1019.
38 P. F. M. Turbiez and J. Roncali., *J. Org. Chem.*, 2003, **68**, 5357–5360.
39 R. G. Nuzzo, E. M. Korenic and L. H. Dubois, *J. Chem.Phys.*, 1990, **93**, 767–773.
40 M. J. Hostetler, J. J. Stokes and R. W. Murray, *Langmuir*, 1996, **12**, 3604–3612.
41 T. Karakouz, A. B. Tesler, T. A. Bendikov, A. Vaskevich and I. Rubinstein, *Adv. Mater.*, 2008, **20**, 3893–3899.
42 H. Skulason and C. D. Frisbie, *Langmuir*, 1998, **14**, 5834–5840.
43 H. Y. Liu, S. G. Liu and L. Echegoyen, *Chem. Commun.*, 1999, 1493–1494.
44 D. F. Perepichka, M. Kondratenko and M. R. Bryce, *Langmuir*, 2005, **21**, 8824–8831.
45 D. F. Perepichka, M. R. Bryce, C. Pearson, M. C. Petty, E. J. L. McInnes and J. P. Zhao, *Angew. Chem., Int. Ed.*, 2003, **42**, 4636–4639.
46 *R. C. Gaussian 03*, M. J. Frisch, G. W. Trucks, H. B. Schlegel, G. E. Scuseria, M. A. Robb, J. R. Cheeseman, J. J. A. Montgomery, T. Vreven, K. N. Kudin, J. C. Burant, J. M. Millam, S. S. Iyengar, J. Tomasi, V. Barone, B. Mennucci, G. S. M. Cossi, N. Rega, G. A. Petersson, H. Nakatsuji, M. Hada, M. Ehara, K. Toyota, R. Fukuda, J. Hasegawa, M. Ishida, T. N., Y. Honda, O. Kitao, H. Nakai, M. Klene, X. Li, J. E. Knox, H. P. Hratchian, J. B. Cross, V. Bakken, C. Adamo, J. J., R. Gomperts, R. E. Stratmann, O. Yazyev, A. J. Austin, R. Cammi, C. Pomelli, J. W. Ochterski, P. Y. Ayala, K. M., G. A. Voth, P. Salvador, J. J. Dannenberg, V. G. Zakrzewski, S. Dapprich, A. D. Daniels, M. C. Strain, O. F., D. K. Malick, A. D. Rabuck, K. Raghavachari, J. B. Foresman, J. V. Ortiz, Q. Cui, A. G. Baboul, S. Clifford, J. C., B. B. Stefanov, G. Liu, A. Liashenko, P. Piskorz, I. Komaromi, R. L. Martin, D. J. Fox, T. Keith, M. A. Al-Laham, C. Y. P., A. Nanayakkara, M. Challacombe, P. M. W. Gill, B. Johnson, W. Chen, M. W. Wong, C. Gonzalez and J. A. P., Gaussian, Inc., Wallingford CT, 2004.

